RESEARCH ARTICLE

Complexation of bis-crown stilbene with alkali and alkaline-earth metal cations. Ultrafast excited state dynamics of the stilbene-viologen analogue charge transfer complex

Valery V. Volchkov[1] (ID) | Mikhail V. Rusalov[1] | Fedor E. Gostev[2] | Ivan V. Shelaev[2] |

Viktor A. Nadtochenko[1,2] | Artem I. Vedernikov[3] | Asya A. Efremova[3] |

Lyudmila G. Kuz'mina[4] | Sergey P. Gromov[1,3] | Michael V. Alfimov[3] | Mikhail Ya. Melnikov[1]

[1] Chemistry Department, M. V. Lomonosov Moscow State University, Moscow, Russian Federation

[2] N. N. Semenov Institute of Chemical Physics, Russian Academy of Sciences, Moscow, Russian Federation

[3] Photochemistry Center, Russian Academy of Sciences, Moscow, Russian Federation

[4] N. S. Kurnakov Institute of General and Inorganic Chemistry, Russian Academy of Sciences, Moscow, Russian Federation

Correspondence
Valery V. Volchkov, Chemistry Department, M. V. Lomonosov Moscow State University, 1-3 Leninskie Gory, Moscow 119991, Russian Federation.
Email: volchkov_vv@mail.ru

Funding information
Russian Science Foundation, Grant/Award Number: Grant 14-13-00076; Russian Foundation for Basic Research, Grant/Award Number: Grant 17-03-00595

Abstract

The complex formation of bis(18-crown-6)stilbene (**1**) and its supramolecular donor-acceptor complex with N,N'-bis(ammonioethyl) 1,2-di(4-pyridyl)ethylene derivative (**2**) with alkali and alkaline-earth metal perchlorates has been studied using absorption, steady-state fluorescence, and femtosecond transient absorption spectroscopy. The formation of $\mathbf{1}M^{n+}$ and $\mathbf{1}(M^{n+})_2$ complexes in acetonitrile was demonstrated. The weak long-wavelength charge-transfer absorption band of **1·2** completely vanishes upon complexation with metal cations because of disruption of the pseudocyclic structure. The spectroscopic and luminescence parameters, stability constants, and 2-stage dissociation constants were calculated. The initial stage of a recoordination process was found in the excited complexes $\mathbf{1}M^+$ and $\mathbf{1}(M^+)_2$ (M = Li, Na). The pronounced fluorescence quenching of **1·2** is explained by very fast back electron transfer ($\tau_{et} = 0.397$ ps). The structure of complex **1·2** was studied by X-ray diffraction; stacked $(\mathbf{1·2})_m$ polymer in which the components were connected by hydrogen bonding and stacking was found in the crystal. These compounds can be considered as novel optical molecular sensors for alkali and alkaline-earth metal cations.

KEYWORDS

back electron transfer, bis-ammonium dipyridylethylene derivative, bis-crown stilbene, donor-acceptor complex, transient absorption, X-ray diffraction

1 | INTRODUCTION

In recent years, reactions involving supramolecular systems based on unsaturated crown compounds, in particular bis(crown ethers), have attracted considerable researchers' attention. Bis(crown ether) compounds, in which 2 macroheterocycles are linked by a flexible aliphatic chain, are known to exhibit higher selectivity and form more stable complexes with alkali and alkaline-earth metal cations than their monocyclic analogues.[1] In some cases, the so-called "molecular tweezers" effect, consisting in selective capture of alkaline-earth metal cations of large diameters, may arise as a result of cooperative action of 2 crown-ether moieties.[2] It was found that binuclear barium complexes of Z isomers of bis(18-crown-6)stilbene (**1**) and bis(18-crown-6)azobenzene can catalyze ethanolysis of esters and anilides via cooperative coordination of

barium ions to the substrate.[3,4] The supramolecular donor-acceptor complexes formed by (E)-**1** and 4,4′-bipyridine, 2,7-diazapyrene, and 1,2-di(4-pyridyl)ethylene derivatives (eg, compounds **2** and **3**) are of considerable interest as model systems for the investigation of the ultrafast photo-induced electron transfer.[5,6] High thermodynamic stability of these complexes ($\log K_s^{1:1}$ of up to 9.42 in MeCN) is due to the coordination of the ammonioalkyl groups to the crown ether moieties of stilbene **1** (see Chart 1). The "structure-property" relationship has been studied for related donor-acceptor complexes, differing in the length of the ammonioalkyl spacers and the type of the central conjugated moiety in the acceptor component.[7,8] It was shown that these complexes can be regarded as fluorescent molecular sensors for alkaline-earth metal cations.

In this study, we established the stoichiometry and studied the stability of complexes formed by stilbene (E)-**1** with alkali and alkaline-earth metal cations as a function of the cation charge density and the content of water in the solution. The stability of complex (E)-**1** with (E)-**2** was studied for dissociation and metal cation substitution reactions. The characteristic times of internal conversion and forward and back diabatic electron transfer were measured by global analysis of the data of femtosecond S_0-S_n absorption dynamics. The dependence of these values on the length of the ammonioalkyl chain of the acceptor was elucidated. The structure of the crystalline complex **1·2** was studied by X-ray diffraction.

2 | EXPERIMENTAL

The structural formulas of compounds **1** to **3** and complex **1·2** are shown in Chart 1. An efficient synthesis of stilbene

(E)-**1**

(E)-**2** (n = 1), (E)-**3** (n = 2)

(E)-**1**·(E)-**2**
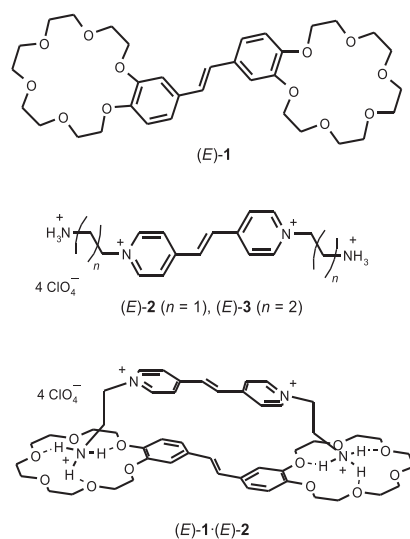
CHART 1 Structures of compounds **1** to **3** and complex **1·2**

1 was developed in Vedernikov et al.[9] The synthesis of acceptor compound **2** and preparation of solid complex **1·2** were described in Gromov et al.[7] The ^{1}H NMR spectra were recorded on a Bruker DRX500 instrument. 18,18′-(E)-Ethene-1,2-diylbis-2,3,5,6,8,9,11,12,14,15-decahydro-1,4,7,10,13,16-benzohexaoxacyclooctadecyne (**1**), ^{1}H NMR (MeCN-d_3, 500.13 MHz, 25°C) δ: 3.58 (s, 8H, 4 CH_2O), 3.58-3.61 (m, 8H, 4 CH_2O), 3.62-3.65 (m, 8H, 4 CH_2O), 3.78 (m, 4H, 2 CH_2CH_2OAr), 3.80 (m, 4H, 2 CH_2CH_2OAr), 4.17 (m, 4H, 2 CH_2OAr), 4.22 (m, 4H, 2 CH_2OAr), 6.92 (d, ^3J = 8.3 Hz, 2H, Ar), 7.03 (s, 2H, HC=CH), 7.05 (dd, ^3J = 8.3, ^4J = 1.9 Hz, 2H, Ar), 7.16 (d, ^4J = 1.9 Hz, 2H, Ar). 4,4′-(E)-Ethene-1,2-diylbis[1-(2-ammonioethyl)pyridinium] tetraperchlorate (**2**) ^{1}H NMR (MeCN-d_3, 500.13 MHz, 25°C) δ: 3.57 (t, ^3J = 6.3 Hz, 4H, 2 CH_2NH$_3$), 4.79 (t, ^3J = 6.3 Hz, 4H, 2 CH_2N), 7.93 (s, 2H, HC=CH), 8.29 (d, ^3J = 6.9 Hz, 4H, Py), 8.76 (d, ^3J = 6.9 Hz, 4H, Py). Complex **1·2** ^{1}H NMR (MeCN-d_3, 500.13 MHz, 25°C) δ: 3.62 (br m, 4H, 2 CH_2NH$_3$), 3.73-4.03 (br m, 36H, 18 CH_2O), 4.29 (br m, 4H, 2 CH_2OAr), 4.65 (br m, 4H, 2 CH_2N), 6.73 (br s, 2H, Ar), 6.94 (s, 2H, ArHC=CHAr), 7.00 (d, ^3J = 8.5 Hz, 2H, Ar), 7.14 (br d, ^3J = 8.5, 2H, Ar), 7.64 (br s, 2H, PyHC=CHPy), 7.84 (br s, 6H, 2 NH$_3$), 7.89 (br d, ^3J = 5.9 Hz, 4H, Py), 8.46 (br d, ^3J = 5.9 Hz, 4H, Py).

Steady-state absorption and fluorescence spectra were recorded at 298 K on a Shimadzu-3100 spectrophotometer and Perkin-Elmer LS-55 and Elumin-2M spectrofluorimeters. The fluorescence quantum yields were determined by comparing the areas under corrected fluorescence spectra of degassed solutions of the samples and quinine bisulfate in 1 N H_2SO_4 (Φ_f = 0.546).[10] The solutions were degassed by bubbling nitrogen through them for 15 minutes.

The details of transient spectra measurements were described in our previous publication.[11] The corrected transient absorption spectra were analyzed by means of the global fitting procedure based on alternating-variable descent method with the assumption of 3-exponential decay kinetics. The global fitting procedure implies that the resulting characteristic times, unlike the pre-exponential factor or the constant term, do not depend on the recording wavelength. The calculation was performed using the set of experimental data for the 430- to 700-nm range and from 0 to 3 ps. The procedure implied minimization of the root-mean-square deviations between the experimental and theoretical data matrix, calculated by variation of the characteristic times τ_i. The calculations were conducted using a script composed of the standard MATLAB 6.0 functions. The errors of τ_i determination are equal to 0.002 ps.

Spectral purity grade (Merck) Li, Na, K, Mg, Ca, and Ba perchlorates were dehydrated by drying in vacuo

(0.01 mm Hg) at 200°C for 5 hours in a VacuCell apparatus. For the dissociation of complexes, we used distilled water purified from traces of salts with a Milli-Q apparatus. All measurements were performed with freshly prepared solutions in spectral grade anhydrous acetonitrile (Cryochrom "0", HPLC grade) at 298 K. The stability constants were calculated using the Equilibrium program based on a multivariable nonlinear least squares method.[12] The average uncertainty amounted to approximately 10%. To avoid the minor dissociation of complex **1·2** caused by traces of water in acetonitrile, the fluorescence spectra of the **1·2**/MeCN/ metal perchlorate system were recorded using solutions of **1·2** with a 20% excess of acceptor **2**.

3 | CRYSTALLOGRAPHY

A single crystal of complex **1·2**·C_6H_6·0.75MeCN·0.5H_2O was coated with perfluorinated oil and mounted on a Bruker SMART-CCD diffractometer (graphite monochromatized Mo-K$_\alpha$ radiation [$\lambda = 0.71073$ Å}, ω scan mode) under a stream of cold nitrogen. The set of experimental reflections was measured, and the structure was solved by direct methods and refined with anisotropic thermal parameters for all nonhydrogen atoms (except for the disordered benzene molecule and the oxygen atoms of the disordered perchlorate anions, which were refined isotropically). The hydrogen atoms were fixed at calculated positions at carbon and nitrogen atoms and then refined using a riding model. The hydrogen atoms of solvate water molecules were not located.

The reflections were collected from a weakly reflecting crystal (mean $I/\sigma(I) = 1.63$). Therefore, the final parameters are characterized by low accuracy. Unfortunately, we failed to obtain better crystals and better structural data. Nevertheless, we include this structure in this article without discussing subtle details of the geometry just to show the arrangement of the donor and acceptor components within the supramolecular complex in the crystalline state.

In the structure of **1·2**·C_6H_6·0.75MeCN·0.5H_2O, 3 of the 4 independent perchlorate anions are each disordered over 2 sites with occupancy ratios of 0.70:0.30, 0.51:0.49, and 0.64:0.36. The C(7)H$_2$ group of the crown ether moiety of **1** is disordered over 2 sites with the occupancy ratio of 0.63:0.37. The conjugated fragment of **2** is disordered with the occupancy ratio of 0.60:0.40. The benzene molecule of solvation is also disordered over 2 close sites with the occupancy ratio of 0.64:0.36. Finally, the acetonitrile molecule and 3 water molecules alternate in the same position of the unit cell, being of 0.75, 0.25, 0.125, and 0.125 occupancies, respectively. SADI, ISOR, AFIX 66,

and DFIX commands were applied to constrain the disordered moieties.

All the calculations were performed using the SHELXL software.[13] CCDC number is 1530014. The data file can be obtained free of charge on application to the CCDC 12 Union Road, Cambridge CB21 EZ, UK. (Fax: (+44) 1223 336 033; email: data_request@ccdc.cam.ac.uk).

4 | RESULTS AND DISCUSSION

4.1 | Ground state complexation and substitution reactions

The addition of alkali and alkaline-earth metal perchlorates to solutions of **1** in acetonitrile induces a short-wavelength shift with a clear-cut isosbestic point in the absorption spectra. Using the isomolar series method, we obtained the stoichiometric coefficients for the complex formation reaction.[14] It can be seen from Figure 1 (inset) that the highest yields of the complexes are attained when the ratio of the bis-crown stilbene **1** and metal cation mole fractions is 0.4:0.6 (2:3). This stoichiometric ratio corresponds to the following 2 reactions taking place in the system:

$$\mathbf{1} + M^{n+} \leftrightarrow \mathbf{1} \cdot M^{n+}, \qquad (1)$$
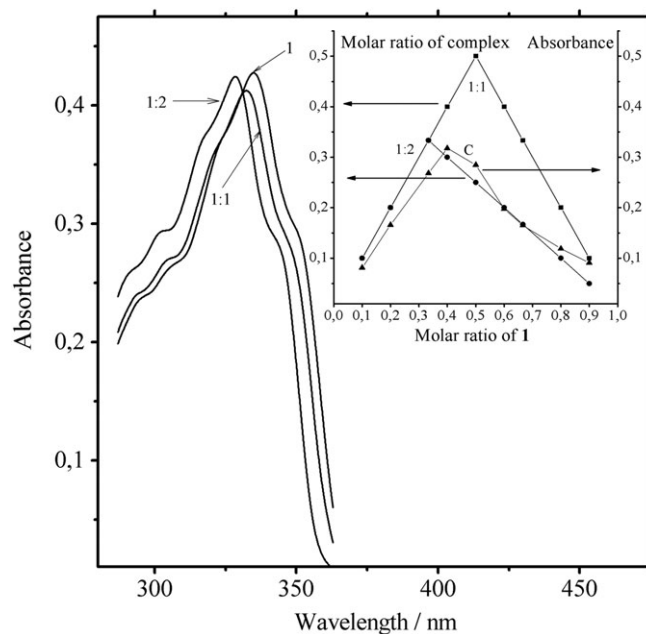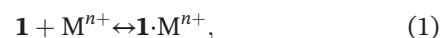
FIGURE 1 Absorption spectrum of **1** (1) and calculated spectra of complexes **1**·Ca^{2+} and **1**·(Ca^{2+})$_2$ in MeCN at 298 K. Inset: Theoretical Job's plots for the irreversible reaction between **1** and Ca^{2+} forming only 1:1 or only 1:2 complexes (left scale) and experimental Job's plot (C, right scale) for the system **1**/MeCN/ $Ca(ClO_4)_2$, $\lambda_{obs} = 320$ nm. (The volume ratios of 1×10^{-4}M solutions of **1** and $Ca(ClO_4)_2$ in MeCN used for absorption measurements were 1:9, 2:8, 1:2, 4:6, 5:5, 6:4, 2:1, 8:2, and 9:1)

$$\mathbf{1}\cdot M^{n+} + M^{n+} \leftrightarrow \mathbf{1}\cdot(M^{n+})_2. \qquad (2)$$
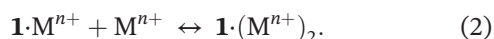
If either only reaction 1 or only the reaction $\mathbf{1} + 2M^{n+} \leftrightarrow \mathbf{1}\cdot(M^{n+})_2$ took place, the maximum of the curve would be attained at 0.5 and 0.33 in the abscissa, respectively. The presence of 2 types of complexes in the system is also supported by the Wallace-Katz method.[15] For the error of 0.002 absorbance units, the absorption spectra have 3 linearly independent components. The spectra of stilbene **1** in acetonitrile, the simulated spectra of complexes $\mathbf{1}\cdot M^{n+}$ and $\mathbf{1}\cdot(M^{n+})_2$, the stability constants $\log K_s^{1:1}$ and $\log K_s^{1:2}$ for reactions 1 and 2, and the extinction coefficients and absorption peaks for the complexes are presented in Figure 1 and in Table 1.

The shifts ($\Delta\lambda_a^{max}$) and extinction coefficients (ε_a^{max}) depend little on the nature of the metal cation. The stability constants are higher for 1:1 complexes than for 1:2 complexes. They increase with increasing cation charge and size match between the cation and the 18-crown-6 ether cavity. The lowest constants were found for the compact Li^+ and Mg^{2+} ions, while the highest ones were inherent in the doubly charged Ba^{2+}, which matches best the size of the 18-crown-6 ether moiety of **1**. The dependence of $\log K_s^{1:1}$ and $\log K_s^{1:2}$ on the charge density is shown in Figure 2 (inset). If the data for Li^+ and Mg^{2+} (the smallest cations) are excluded from consideration, the function becomes linear. Similar low $\log K_s$ values have been observed for the reaction of Li^+ with 4-*N*-tetraoxaaza-15-crown-5 benzothiazole derivative and were attributed to metal ion coordination to only 4 oxygen atoms of the macrocycle, the remaining 2 vacancies in the lithium coordination sphere being filled by counter-ion oxygen atoms and/or solvent molecules.[16] A similar trend was identified in a study of complex formation of benzo-18-crown-6 ether and *N*-phenylaza-18-crown-6
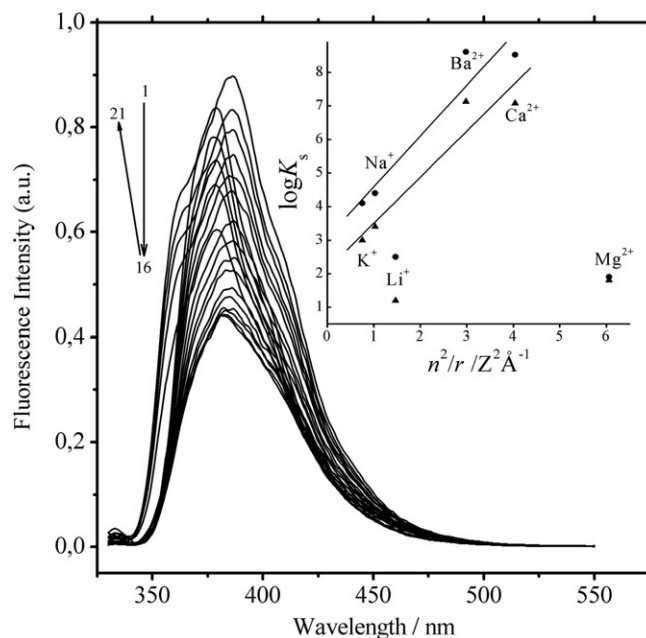
FIGURE 2 Corrected fluorescence spectra of **1** (~1 × 10^{-5}M) in MeCN at 298 K at different concentration of Ba^{2+} ions.
[Ba(ClO₄)₂]: 0 (1), 1.11 × 10^{-6} (2), 2.20 × 10^{-6} (3), 3.28 × 10^{-6} (4), 4.35 × 10^{-6} (5), 5.40 × 10^{-6} (6), 6.45 × 10^{-6} (7), 7.46 × 10^{-6} (8), 8.51 × 10^{-6} (9), 9.52 × 10^{-6} (10), 1.05 × 10^{-5} (11), 1.15 × 10^{-5} (12), 1.25 × 10^{-5} (13), 1.35 × 10^{-5} (14), 1.44 × 10^{-5} (15), 1.54 × 10^{-5} (16), 1.82 × 10^{-5} (17), 2.09 × 10^{-5} (18), 2.35 × 10^{-5} (19), 2.61 × 10^{-5} (20), and 2.86 × 10^{-5} M (21). Inset: $\log K_s^{1:1}$ (●) and $\log K_s^{1:2}$ (▲) of **1** as a function of charge density

ether derivatives with alkali metal cations.[17,18] Apparently, in our case, too, the main cause of the low stability of Li^+ and Mg^{2+} complexes of **1** is a sharp size mismatch between the cation and the 18-crown-6 ether cavity of **1**.

Alkali and alkaline-earth metal perchlorates can not only react with free macrocyclic moieties of compound **1** but also displace the coordinated ammonium ions from them in complexes of type $\mathbf{1}\cdot\mathbf{2}$.[7,8] Indeed, upon the

TABLE 1 Absorption maximum wavelengths (λ_a^{max}), extinction coefficients at the absorption maxima (ε_a^{max}), stability ($\log K_s$) and dissociation ($\log K_a$)[a] constants for $\mathbf{1}M^{n+}$ and $\mathbf{1}(M^{n+})_2$ in MeCN at 298 K, and metal cation diameters

Salt	λ_a^{max} (1:1), nm	λ_a^{max} (1:2), nm	$\varepsilon_a^{max} \times 10^{-4}$ (1:1), M^{-1} cm^{-1}	$\varepsilon_a^{max} \times 10^{-4}$ (1:2), M^{-1} cm^{-1}	$\log K_s^{1:1}$, M^{-1}	$\log K_s^{1:2}$, M^{-1}	$\log K_a^{1:2}$, M^{-1}	$\log K_a^{1:1}$, M^{-1}	Diameter of Cation, Å
LiClO₄	334	332	3.50	3.60	2.5	1.2	0.9	0.1	1.36
NaClO₄	334	333.5	3.50	3.61	4.4	3.4	1.07	0.2	1.94
KClO₄	333	333	3.61	3.61	4.1	3.0	1.3	1.3	2.66
Mg(ClO₄)₂	332.5	328	3.64	3.40	1.9	1.8	0.5	0.2	1.32
Ca(ClO₄)₂	332	328.5	3.50	3.64	8.5	7.1	1.8	1.2	1.98
Ba(ClO₄)₂	334	329	3.46	3.64	8.6	7.1	1.2	0.3	2.68

[a]All dissociation constants were calculated for the solutions **1**/MeCN/0.001M metal perchlorate, excluding **1**/MeCN/0.05M Mg(ClO₄)₂ system. The average uncertainty amounted to approximately 10%.

λ_a^{max} of **1** in MeCN = 336 nm, $\varepsilon_a^{max} = 3.57 \times 10^4$ M^{-1} cm^{-1}.

λ_a^{max} of $\mathbf{1}\cdot\mathbf{2}$ in MeCN = 319 and 535 nm (CT band), $\varepsilon_a^{max} = 6.54 \times 10^4 M^{-1}$ cm^{-1}, and $\varepsilon_a^{max} = 308$ M^{-1} cm^{-1} (CT band).

$\log K_a^{1:2} = 1.5$, $\log K_a^{1:1} = 0.2$ (2-step dissociation constants for $\mathbf{1}\cdot\mathbf{2}$).

addition of Li, Na, K, Mg, Ca, and Ba perchlorates, the absorption spectra of $1·2$ in acetonitrile show a minor long-wavelength shift accompanied by intensity increase and appearance of a clear isosbestic point (Figure 3). However, even with excess metal salt, the absorption peaks in these systems (324-325 nm) do not reach values characteristic of the $1·(M^{n+})_2$ complexes (Table 1). With an error of 0.002 absorbance units, the absorption spectra of the systems, except for $1·2/KClO_4$, contain 2 linearly independent components. This is indicative of a substitution reaction involving only one metal cation and detachment of one ammonioethyl spacer in the complex $1·2$:

$$1·2 + M^{n+} \leftrightarrow 2·1·M^{n+}. \qquad (3)$$

The possibility of simultaneous dissociation involving the second ammonioethyl spacer is still an open question. The constants for replacement of $1·2$ by the 1:1 complex of 1 with the metal cation calculated with a correlation coefficient of >0.998 are summarized in Table 2. Their dependence on the type of cation is similar to that for complexation of free 1. More intense absorption band of complex $1·2$ ($\lambda_a^{max} = 319$ nm, $\varepsilon_a^{max} = 35\ 700 M^{-1}\ cm^{-1}$) is shifted to shorter wavelengths with respect to the arithmetic sum of the absorption bands of 1 and 2 taken in an equimolar ratio. The spectrum of the complex also
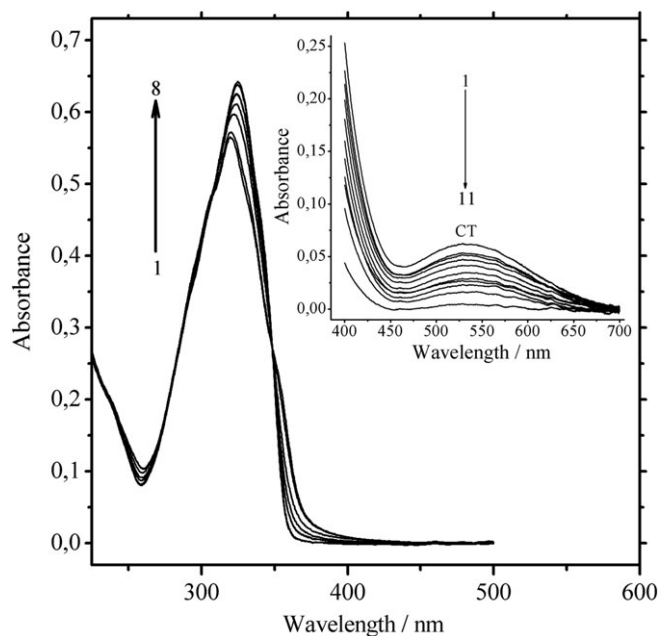
FIGURE 3 Absorption spectra of $1·2$ (~1×10^{-5}M) in MeCN at 298 K. Ba(ClO$_4$)$_2$: 0 (1), 3.66×10^{-6} (2), 1.09×10^{-5} (3), 1.44×10^{-5} (4), 1.79×10^{-5} (5), 2.14×10^{-5} (6), 3.15×10^{-5} (7), and 6.94×10^{-4} M (8). Inset: Absorption spectra of CT band of $1·2$ (2.0×10^{-4}M) in MeCN at 298 K. [Ba(ClO$_4$)$_2$]: 0 (1), 2.75×10^{-5} (2), 5.44×10^{-5} (3), 8.10×10^{-5} (4), 1.07×10^{-4} (5), 1.33×10^{-4} (6), 1.58×10^{-4} (7), 1.83×10^{-4} (8), 2.07×10^{-4} (9), 2.32×10^{-4} (10), and 3.02×10^{-4}M (11)

exhibits a much weaker charge transfer band ($\lambda_a^{max} = 535$ nm, $\varepsilon_a^{max} = 308$ M^{-1} cm^{-1}). As the metal perchlorate concentration in the solution increases, the contribution of the charge transfer band gradually decreases as a result of destruction of the pseudocyclic donor-acceptor complex structure (Figure 3, inset).

4.2 | Dissociation

To estimate the stability of complexes 1 upon variation of the parameters of the medium and to find the appropriate water content in the solvent for efficient complexation, it is necessary to determine the quantitative characteristics of their dissociation. For this purpose, we used the standard spectrophotometric titration procedure. In all cases, with increasing content of water, the absorption band of complex $1(M^{n+})_2$ decreased, with restoration of, first, the absorption band of $1M^{n+}$ and then the band of free bis-crown stilbene. For obtaining admissible dissociation constants, we will describe the process by reactions 4 and 5, which do not include the solvated metal cation.

$$1·(M^{n+})_2 + n_1 H_2O \leftrightarrow 1·M^{n+}, \qquad (4)$$

$$1·M^{n+} + n_2 H_2O \leftrightarrow 1. \qquad (5)$$
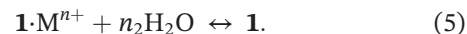
Because of substantial superposition of the absorption bands for 1 and its complexes, the dissociation constants $K_a^{1:1}$ and $K_a^{1:2}$ were calculated from Equation 6 derived on the basis of the modified Ketelaar equation for $n + 1$-order reactions.[19] The equation was derived with the assumption that the extinction coefficients of 1:1 and 1:2 complexes in the absorption maximum of bis-crown stilbene are equal ($\varepsilon_\lambda^{1(M)2} \approx \varepsilon_\lambda^{1M}$).

$$\frac{1}{\varepsilon_\lambda^{Obs} - \varepsilon_\lambda^{1(M)_2}} = \frac{1}{\varepsilon_\lambda^{1} - \varepsilon_\lambda^{1(M)_2}} + \frac{1}{\left(\varepsilon_\lambda^{1} - \varepsilon_\lambda^{1(M)_2}\right)} \frac{1 + K_a^{1:1}[H_2O]^{n_1}}{K_a^{1:1} K_a^{1:2}[H_2O]^{n_1+n_2}}, \qquad (6)$$

where $\varepsilon_\lambda^{Obs}$ is the experimental extinction coefficient (the ratio of the observed absorbance in the absorption maximum of 1 to the initial concentration of the 1:2 complex), ε_λ^{1} and $\varepsilon_\lambda^{1(M)2}$ are the extinction coefficients of 1 and the 1:2 complex at the absorption maximum wavelength of bis-crown stilbene, and n_1 and n_2 are the numbers of water molecules involved in the reactions. The $\varepsilon_\lambda^{1(M)2}$ values were calculated using the limiting absorption spectra of the 1:2 complexes calculated using the Equilibrium software. In all cases, the best fit to Equation 6 was achieved for $n_1 = n_2 = 1$ (Figure 4).

TABLE 2 Fluorescence maximum wavelengths (λ_f^{max}), quantum yields (Φ_f), Stokes shifts for complexes $1M^{n+}$ and $1(M^{n+})_2$, and substitution constants ($\log K_s$) for complex $1 \cdot 2$ by metal perchlorate in MeCN at 298 K[a]

Salt	λ_f^{max} 1:1/1:2, nm	Φ_f^{max} 1:1/1:2, nm	ν_f^{max} (1) $-$ ν_f^{max} (complex) 1:1/1:2, cm^{-1}	Stokes shift, ν_a^{max} (complex) $-$ ν_f^{max} (complex) 1:1/1:2, cm^{-1}	$\log K_s$, M^{-1}
LiClO$_4$	385/–	0.29/–	30/–	4287/–	1.1
NaClO$_4$	383/382.5	0.25/0.5	$-183/-272$	3941/3897	3.2
KClO$_4$	383/381	0.24/0.47	$-273/-349$	3942/3877	3.6
Mg(ClO$_4$)$_2$	385/377	0.19/0.43	$-9/-694$	4229/3975	1.5
Ca(ClO$_4$)$_2$	382/378	0.15/0.35	$-77/-562$	4198/3960	7.1
Ba(ClO$_4$)$_2$	381/379	0.16/0.34	$-225/-491$	3858/4059	5.3

[a]For **1** in MeCN: λ_f^{max} = 386 nm, Φ_f = 0.400, Stokes shift = 3935 cm^{-1}. The average uncertainty for K_s and Φ_f^{max} amounted to approximately 10%.

The 2-step dissociation constants are summarized in Table 1. It can be easily seen that they are substantially lower than the corresponding complexation constants and depend on the cation nature in a similar way. The reaction of $1 \cdot 2$ with water gives rise, first, to an absorption band with a peak at 323 nm and then to a long-wavelength shoulder at 336 nm, which is indicative of stepwise dissociation with detachment of both ammonioethyl groups. The dissociation constants of $1 \cdot 2$ are given in the note to Table 2.

4.3 | Steady-state fluorescence spectroscopy

Investigation of the fluorescence behavior of the complexes upon permanent excitation provides more data
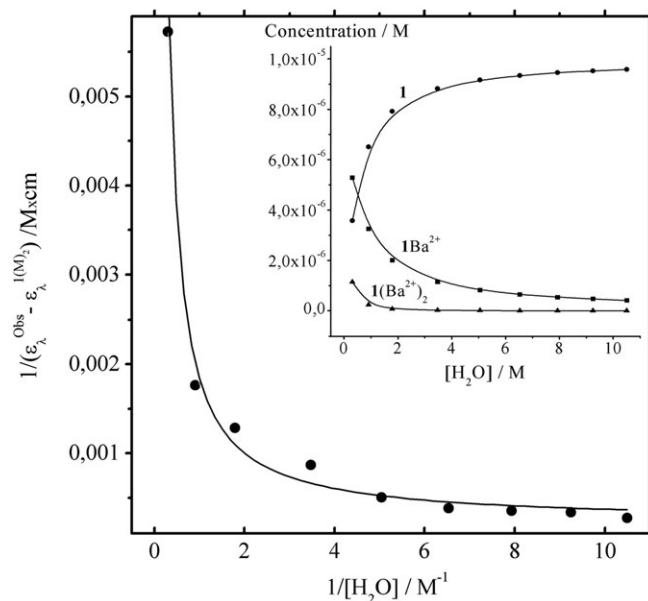
FIGURE 4 Two-step dissociation of complexes in the system approximately 1 × 10^{-5} M **1**/MeCN/10^{-3}M Ba(ClO$_4$)$_2$/H$_2$O. Fitting to Equation 6, [H$_2$O]:: 0.31, 0.91, 1.79, 3.47, 5.05, 6.53, 7.93, 9.25, 10.50, and 11.69 M. Inset: Concentration curves for **1** and its complexes

about the stoichiometry of the complexation and dissociation reactions, the presence of the dynamic component, and the degree of charge transfer upon excitation and also reveals the signs of light-induced recoordination and back electron transfer. A vivid example confirming the stoichiometry of complexation can be seen in Figure 2. Here, with increasing salt concentration, fluorescence of **1** is first quenched and then the quenching stops and is replaced by fluorescence enhancement with a noticeable short-wavelength shift (in all cases, the excitation was performed in isosbestic points). On the subsequent addition of water, the spectra shift strictly in the inverse sequence with restoration of the fluorescence of **1**. These observations are fully consistent with the conclusions drawn from analysis of the changes in the absorption spectra. The spectroscopic and luminescence parameters of complexes $1M^{n+}$ and $1(M^{n+})_2$, the fluorescence quantum yields, and the Stokes shifts calculated using the Equilibrium software are summarized in Table 2. It can be seen from the table that complex $1M^{n+}$ shows a weaker fluorescence than $1(M^{n+})_2$, which is attributable to more uniform distribution of electron density in the symmetric structure of the latter. The fluorescence Stokes shifts of the complexes are relatively small. In the case of Na$^+$ and Li$^+$, the shifts of the fluorescence peaks upon the formation of 1:2 complexes are 1 and 3 nm smaller than the shifts of the absorption peaks. This suggests the occurrence of an early stage of light-induced recoordination (ie, cleavage of the ArO···M$^+$ coordination bond in the excited state). Other systems exhibit no signs of light-induced recoordination. The fluorescence quantum yield of $1 \cdot 2$ is <0.001, which is typical of back electron transfer. The addition of metal perchlorates to a solution of $1 \cdot 2$ in acetonitrile brings about gradual enhancement of fluorescence, resulting from decomposition of the donor-acceptor complex in the substitution reaction to give complexes $1M^{n+}$ and $1(M^{n+})_2$. Although the obtained quantum yields (0.115 for Na$^+$ and 0.086 for Li$^+$) do not reach the values found for $1 \cdot (M^{n+})_2$, the

fluorescence maxima correspond to them. This suggests dynamic detachment of the second ammonioethyl spacer in the hypothetical complex $2 \cdot 1M^{n+}$ to be replaced by a metal cation. These conclusions are in line with the results obtained for similar complex $1 \cdot 3$.[5]

4.4 | Transient absorption spectroscopy

It is known that with a realistic kinetic scheme at hand, application of the global fitting procedure to the data of transient absorption spectroscopy allows one to calculate the species-associated spectra with the species lifetimes, which characterize the steps of conversion from the Franck-Condon state of the molecule. If no other processes are superimposed on the charge phototransfer in this time span, isosbestic points can be observed in the transient absorption spectra. We used $1(Ba^{2+})_2$ for the comparison with 1, as barium perchlorate forms highly stable complexes with crown ethers and does not tend to absorb water. The differential optical densities $\Delta D(\lambda, t)$ of 1 in acetonitrile, either free or fully complexed with Ba^{2+}, and also of complex $1 \cdot 2$ were measured after excitation by 30 fs, 330-nm (near the isosbestic point) pump pulse in the time window of 500 ps. The transient absorption variation of $1 \cdot 2$ on the femtosecond-picosecond time scale in the 400- to 650-nm range is shown in Figure 5. The short-wavelength edge of the spectra of all 3 samples (400-450 nm) shows a stable bleaching signal. The evolution of the spectra of free ligand and complex $1(Ba^{2+})_2$ can be described as follows. In the range from 0.5 to 1 ps in the case of 1 and from 0.3 to 1 ps in the case of $1(Ba^{2+})_2$, absorption rapidly increases to form a single broad band at 561 and 568 nm, respectively. In the range from 1 to 500 ps, this band does not noticeably change. Three stages can be distinguished in the spectral kinetics of complex $1 \cdot 2$ upon excitation in the principal absorption band (330 nm). During the first 0.3 ps, the band with a peak at 528 nm is transformed into a shorter-wavelength band of equal intensity with a peak at 495 nm. Then it gradually decays in the range below 3 ps and forms a low-intensity band at 555 nm on its long-wavelength side (Figure 5). The position and intensity of the band do not change in the range from 3 to 500 ps.

The obtained results can be interpreted in the following way. Although the kinetics of 1 and $1(Ba^{2+})_2$ are similar, the resultant spectra of free ligand and the complex are not identical, which is indicative of the absence of Ba^{2+} photoejection into the solution. Nevertheless, the long-wavelength S_1-S_n absorption maximum of $1(Ba^{2+})_2$ attests to weakening of the $ArO \cdots Ba^{2+}$ bonds in the excited complex. The pattern of evolution of the spectra of complex $1 \cdot 2$ generally corresponds to
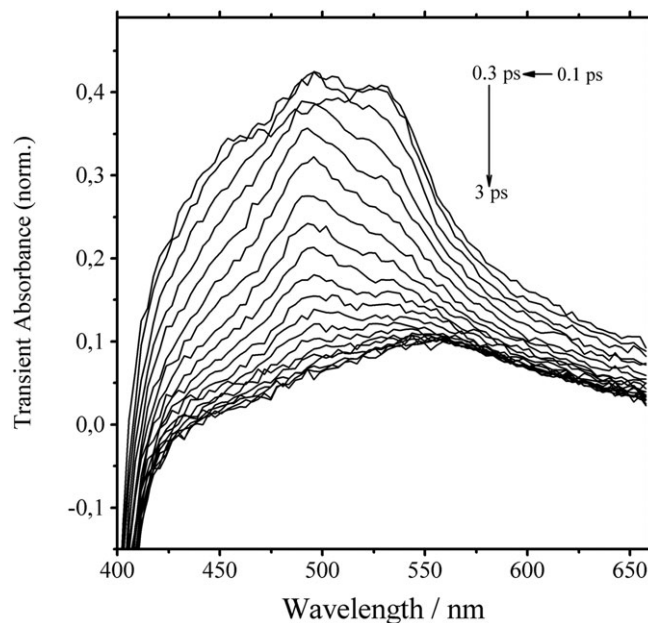
FIGURE 5 Differential absorption of $1 \cdot 2$ (~1.0×10^{-4}M) in MeCN within 0.1 to 3 ps after excitation with a 30-fs pulse at 330 nm. The time increment is 0.1 ps

the data obtained for the analogous complex $1 \cdot 3$.[5] In the case of $1 \cdot 3$, the characteristic spectral reshaping is also present in the range of 0.12 to 0.3 ps with the subsequent decay of the band formed in the range from 0.3 to 3.4 ps. The difference is in the formation of a clear-cut band at 555 nm for $1 \cdot 2$, which, unlike the reported data, does not decay with time.[5] The decay kinetics of the transient absorption band, peaking at 495 nm in the 0.3- to 3-ps range, is as follows. With the use of the global fitting procedure as applied to the whole set of data in the range from 430 to 700 nm, this band is adequately described by 3 exponents of the form $\Delta D(\lambda, t) = A_0(\lambda) + A_1(\lambda) \times \exp(-t/0.079) + A_2(\lambda) \times \exp(-t/0.289) + A_3(\lambda) \times \exp(-t/0.397)$. As an illustration, Figure 6 shows the curves that describe the decay kinetics of complex $1 \cdot 2$ at the front, peak, and decline of the spectrum and the obtained spectral dependences of the pre-exponential factors A_0 to A_3 (Figure 6, inset).

It is known that the applicability of a proposed fitting curve can, in particular, be evaluated on the basis of the autocorrelation function of residuals,[20] specifically, the scattering of the experimental points around this function must be random. As can be seen in Figure 6B, the absence of the clearly defined waves in the autocorrelation function attests to the admissibility of the proposed description. The shortest kinetic component refers to the internal conversion $S_n \rightarrow LE$, the intermediate component corresponds to the direct electron transfer $LE \rightarrow CT$ followed by relaxation to the lower CT state, and the last component refers
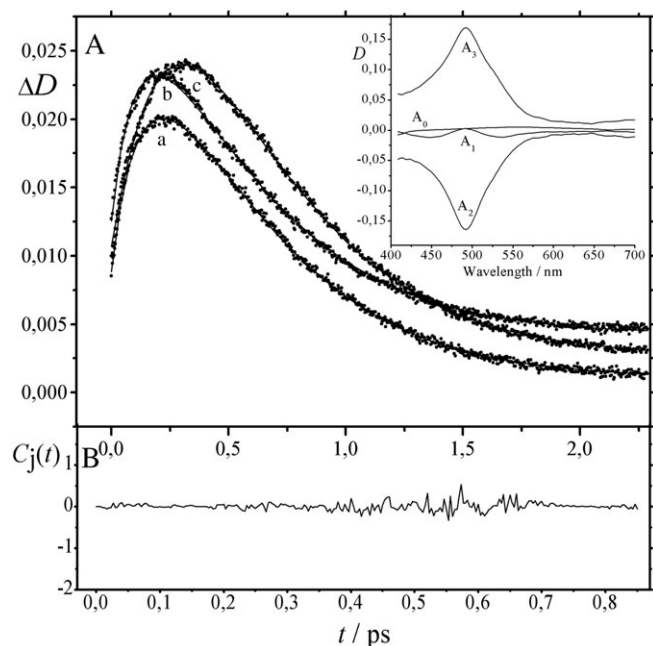
FIGURE 6 Time plot of the transient absorption spectra of **1·2** (~1.0×10^{-4}M) (A) at 466 nm (a), 495 nm (b), and 526 nm (c) in the 0- to 2.3-ps range. The smooth curves are from global fitting to the 3-exponential model: $y = A_0(\lambda) + A_1(\lambda) \times \exp(-t/0.079) + A_2(\lambda) \times \exp(-t/0.289) + A_3(\lambda) \times \exp(-t/0.397)$. Inset: Wavelength-dependent pre-exponential factors. Autocorrelation function of residues (B) obtained for the kinetic curves at 495 nm (maximum)

to the back electron transfer CT $\rightarrow$ S_0. The spectral reshaping observed in the short-wavelength range can reflect not only photorelaxation from higher excited states but also the light-induced recoordination of the NH_3^+ groups connected to the macrocycles of **1**. Apparently, here, light-induced recoordination implies a decrease in the degree of displacement of the lone electron pairs of oxygen, hydrogen bonded to the ammonium ion, and restoration of the contribution of these lone pairs to the conjugation chain of bis-crown stilbene. The characteristic times found for the analogue **1·3** are as follows: 0.150, 0.295, and 0.536 ps.[5] Thus, we observe a decrease in all 3 relaxation times with decreasing length of ammonioalkyl spacers of the acceptor. Apparently, this is a consequence of the closer positions of the conjugated moieties of the donor and acceptor components in complex **1·2** in comparison with **1·3** due to shorter ammonioethyl group.

4.5 | X-ray diffraction analysis

We succeeded in growing the single crystals of complex **1·2** by slow saturation of its acetonitrile solution with benzene vapor at room temperature and performed

X-ray diffraction study. The X-ray experiment results and refinement details are summarized in Table S1. The structure of the main components of the complex is shown in Figure 7.

Apart from the main components, the independent part of the unit cell was found to contain highly disordered 4 perchlorate anions and disordered solvation molecules of benzene, MeCN, and water. The considerable disorder of all crystal components decreases the crystal reflectivity and, hence, reduces the accuracy of X-ray diffraction experiment.

The conjugated moiety of di(4-pyridyl)ethylene derivative **2** is disordered over 2 conformations with site occupancy ratio of 0.60:0.40. The conjugated moieties of both complex components are nearly planar: The dihedral angle between the benzene ring planes in the molecule of **1** is only 5.7(2)° and the pyridine rings in **2** are twisted by only 5.4(4)° and 6.6(7)° for the predominant and minor conformers, respectively. The mean planes of the conjugated moieties of the donor and acceptor components cross at an angle of 7.4(1)°. Thus, the nearly parallel arrangement of the conjugated moieties at approximately 3.5 Å distance and considerable overlap of their projections in the structure of **1·2**·C_6H_6·0.75MeCN·0.5H_2O give rise to effective intermolecular charge transfer donor-acceptor interactions responsible for the full, nearly black color of the crystal. The studied single crystal of **1·2** C_6H_6·0.75MeCN·0.5H_2O had a stacked packing mode for the main components (Figure 8). Instead of the relatively isolated pseudocyclic complexes **1·2**, which exist in dilute solutions (see Chart 1), infinite stacks $(\mathbf{1·2})_m$ composed of alternating hydrogen-bonded donor and acceptor molecules are formed in the crystal. This crystal packing is predetermined by the orientation of the ammonioethyl *N*-substituents of compound **2** on different sides of the conjugated moiety plane. Apparently, the distance between the ammonium groups of **2** does not fully match the distance between the centers of the macrocycles of **1** as needed for the formation of pseudocyclic complexes **1·2** that could form a close packing in the crystal. Alternatively, the formation of **1·2** may be not beneficial for effective stacking interactions between the neighboring complexes in the crystal cell. The macrocyclic moieties of **1** in the crystal form a typical round (crown-like) conformation, which is most favorable for binding the primary ammonium ions. The ammonium groups of compound **2** form directional ($N(1)H_3^+$) or bifurcated ($N(4)H_3^+$) hydrogen bonds with the oxygen atoms of the 18-membered macrocycles. The $N(1)H$...$O(1,3,5)$ distances are in the range of 1.90 to 2.08 Å, the angles at the H atoms are 146° to 175°, whereas the $N(4)$H...O(macrocycle) distances are somewhat longer, 2.05 to 2.21 Å, and the corresponding angles are smaller,
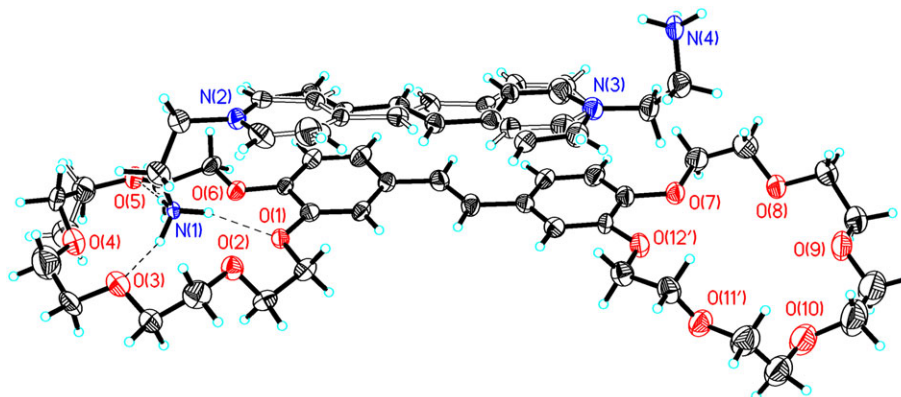
FIGURE 7 Structure of the main components of complex $1 \cdot 2 \cdot C_6H_6 \cdot 0.75MeCN \cdot 0.5H_2O$. Thermal ellipsoids are drawn at the 30% probability level. Hydrogen bonds are shown by dash lines. The minor components of the disorder are shown with hollow bonds
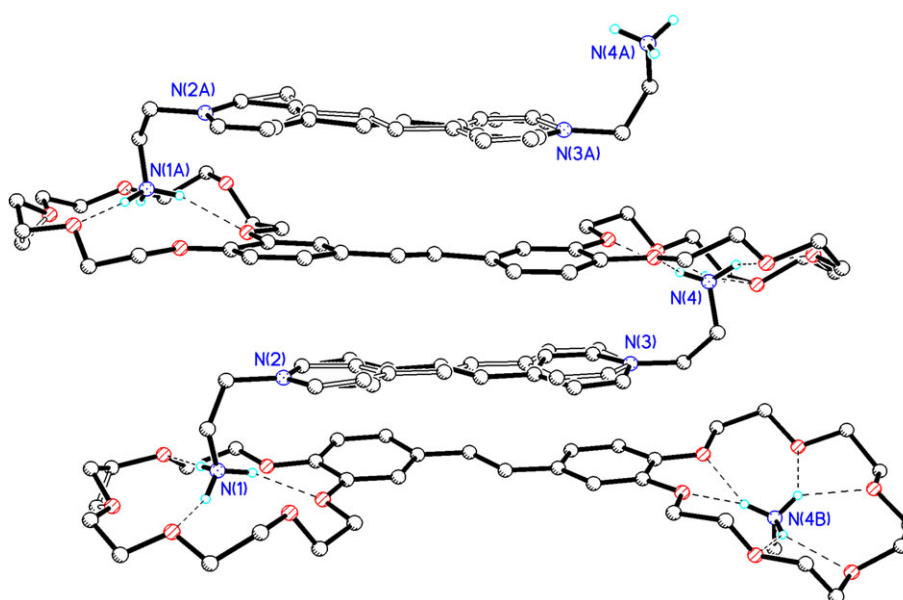
FIGURE 8 Stack of the donor and acceptor molecules in the crystal $1 \cdot 2 \cdot C_6H_6 \cdot 0.75MeCN \cdot 0.5H_2O$. Hydrogen bonds are drawn with dash lines. Most of hydrogen atoms are not shown for clarity. The additional letters "A" and "B" indicate that the atoms are in symmetrically related positions

126° to 144°. These parameters correspond to medium-strength hydrogen bonds.

5 | CONCLUSIONS

The reaction of (*E*)-bis(18-crown-6)stilbene (**1**) with the Li$^+$, Na$^+$, K$^+$, Mg^{2+}, Ca^{2+}, and Ba^{2+} ions in acetonitrile gives rise to 1:1 and 1:2 complexes. The substitution reaction between the donor-acceptor complex **1** with (*E*)-1,2-di(4-pyridyl)ethylene derivative **2** and the Li$^+$, Na$^+$, Mg^{2+}, Ca^{2+}, and Ba^{2+} ions induces detachment of one ammonioethyl spacer to give a complex incorporating one metal cation (**2·1**M^{n+}). The absorption spectra of complexes **1**M^{n+} and **1**(M^{n+})$_2$ show a hypsochromic shift with respect to the spectra of free **1** and a minor

bathochromic shift with respect to the spectrum of ccomplex **1·2**. The stability constants of 1:1 and 1:2 complexes generally obey a linear dependence on the metal cation charge density. The highest logK_s values were noted for complexes of **1** with Ba^{2+}, which match most closely the 18-crown-6 ether cavity. All of the complexes undergo stepwise dissociation in the presence of water. The excited complexes of **1** with Li$^+$ and Na$^+$ show the initial stage of light-induced recoordination. A decrease in the 3 characteristic relaxation times of complex **1·2** with decreasing length of the ammonioalkyl *N*-substituents of the acceptor was demonstrated by femtosecond differential absorption spectroscopy. According to X-ray diffraction, a stacked polymer $(1 \cdot 2)_m$ rather than relatively isolated pseudocyclic complexes **1·2** is formed in the crystal.

ACKNOWLEDGEMENTS

ORCID

Valery V. Volchkov http://orcid.org/0000-0002-9902-076X

REFERENCES

[1] K. Kimura, T. Shono, in *Cation Binding by Macrocycles. Complexation of Cationic Species by Crown Ethers*, (Eds: Y. Inoue, G. W. Gokel), Marcel Dekker, New York, USA **1990**, Ch. 10.

[2] E. N. Ushakov, S. P. Gromov, O. A. Fedorova, Y. V. Pershina, M. V. Alfimov, F. Barigelletti, L. Flamigni, V. Balzani, *J Phys Chem A* **1999**, *103*, 11188.

[3] R. Cacciapaglia, S. Di Stefano, L. Mandolini, *J Org Chem* **2002**, *67*, 521.

[4] R. Cacciapaglia, S. Di Stefano, L. Mandolini, *J. Am. Chem. Soc.* **2003**, *125*, 2224.

[5] E. N. Ushakov, V. A. Nadtochenko, S. P. Gromov, A. I. Vedernikov, N. A. Lobova, M. V. Alfimov, F. E. Gostev, A. N. Petrukhin, O. M. Sarkisov, *Chem. Phys.* **2004**, *298*, 251.

[6] E. N. Ushakov, S. P. Gromov, A. I. Vedernikov, E. V. Malysheva, A. A. Botsmanova, M. V. Alfimov, B. Eliasson, U. G. Edlund, J. K. Whitesell, M. A. Fox, *J Phys Chem* **2002**, *106*, 2020.

[7] S. P. Gromov, A. I. Vedernikov, E. N. Ushakov, N. A. Lobova, A. A. Botsmanova, L. G. Kuz'mina, A. V. Churakov, Y. A. Strelenko, M. V. Alfimov, J. A. K. Howard, et al., *New J. Chem.* **2005**, *29*, 881.

[8] A. I. Vedernikov, E. N. Ushakov, A. A. Efremova, L. G. Kuz'mina, A. A. Moiseeva, N. A. Lobova, A. V. Churakov, Y. A. Strelenko, M. V. Alfimov, J. A. K. Howard, et al., *J Org Chem* **2011**, *76*, 6768.

[9] A. I. Vedernikov, S. S. Basok, S. P. Gromov, L. G. Kuz'mina, V. G. Avakyan, N. A. Lobova, E. Y. Kulygina, T. V. Titkov, Y. A. Strelenko, E. I. Ivanov, et al., *Russ. J. Org. Chem.* **2005**, *41*, 843.

[10] W. H. Melhuish, *J Phys Chem* **1961**, *65*, 229.

[11] V. V. Volchkov, F. E. Gostev, I. V. Shelaev, V. A. Nadtochenko, S. N. Dmitrieva, S. P. Gromov, M. V. Alfimov, M. Ya. Melnikov, *J Fluoresc* **2016**, *26*, 585.

[12] D. M. Himmelblau, *Applied Nonlinear Programming*, Mc-Grow-Hill, Austin, USA **1972**.

[13] G. M. Sheldrick, *Acta Crystallogr C* **2015**, *71*, 3.

[14] P. Job, *Ann. Chim.* **1928**, 9,113.

[15] R. M. Wallace, S. M. Katz, *J Phys Chem* **1964**, *68*, 3890.

[16] K. Rurack, J. L. Bricks, G. Reck, R. Radeglia, U. Resch-Genger, *J Phys Chem A* **2000**, *104*, 3087.

[17] S. P. Gromov, A. I. Vedernikov, E. N. Ushakov, L. G. Kuz'mina, A. V. Feofanov, V. G. Avakyan, A. V. Churakov, Y. S. Alaverdyan, E. V. Malysheva, M. V. Alfimov, J. A. K. Howard, B. Eliasson, U. G. Edlund, *Helv. Chim. Acta* **2002**, *85*, 60.

[18] S. N. Dmitrieva, M. V. Churakova, N. A. Kurchavov, A. I. Vedernikov, A. Ya. Freidzon, S. S. Basok, A. A. Bagatur'yants, S. P. Gromov, *Russ. J. Org. Chem.* **2011**, *47*, 1101.

[19] J. A. A. Ketelaar, C. Van De Stolpe, A. Goudsmit, W. Dzcubas, *Rec Trav Chim Pays-Bas* **1952**, *71*, 1104.

[20] A. Grinvald, I. Z. Steinberg, *Anal. Biochem.* **1974**, *59*, 583.

SUPPORTING INFORMATION

Additional Supporting Information may be found online in the supporting information tab for this article.